ISSN: 1231-4005
e-ISSN: 2354-0133
DOI: 10.5604/01.3001.0010.2909

PROPELLER OPTIMIZATION FOR SMALL UNMANNED AERIAL VEHICLES

Tom Kusznir, Jarosław Smoczek

AGH University of Science and Technology
Faculty of Mechanical Engineering and Robotics
30 Mickiewicza Av. 30, 30-059 Krakow, Poland
e-mail: tkusznir@agh.edu.pl, smoczek@agh.edu.pl

Abstract

Small-unmanned aerial vehicle propellers usually have a low figure of merit due to operating in the low Reynold's number region due to their size and velocity. The airflow on the airfoil becomes increasingly laminar in this region thus increasing the profile drag and consequently reducing the figure of merit of the rotor. In the article, the airfoil geometries are parameterized using the Class/Shape function transformation. Particle swarm optimization is used to design an airfoil, operating in a Reynolds number of 100,000, which has a high lift to drag ratio. To avoid exceeding geometric constraints of the airfoil, a deterministic box constraint is added to the algorithm. The optimized airfoil is then used for a preliminary design of a rotor; given some design, constraints on the tip chord the rotor radius and the blade root chord, with parameters that achieve the highest theoretical figure of merit. The rotor parameters are obtained using a combination of momentum theory and blade element theory. The figure of merit of an optimal propeller with the same geometric parameters is then compared using the optimized airfoil and the Clark Y airfoil. The optimization is done in MATLAB while the aerodynamic coefficients are obtained from XFOIL. The results of the numerical simulation are presented in the article.

Keywords: *unmanned aerial vehicles, particle swarm optimization, airfoil modelling*

1. Introduction

The use of small-unmanned aerial vehicles (sUAV) has been growing rapidly in recent years with applications ranging from professional aerial surveying to recreational use. The small size puts a limitation on their load capacity, and consequently on their power source, which in turn adds a constraint on flight time. One method to increase flight time is to increase the aerodynamic efficiency of the propellers.

Due to the nature of small unmanned aerial vehicles (sUAVs), the airfoils typically operate in low Reynolds number regions ($<5\cdot10^5$). In this region, the flow becomes increasingly laminar causing an increase in aerodynamic drag, and as a result reduces the aerodynamic efficiency of the propeller [1, 17]. The general method of increasing the efficiency of rotors has been well studied. It has developed using blade element momentum theory (BEMT). This method in combination with airfoil optimization, increasing the lift and reducing the drag, results in a propeller with a higher figure of merit (FoM) in comparison to other propellers operating in the low Reynolds number region.

Metaheuristic optimization, such as particle swarm optimization (PSO), is suitable for optimization of airfoils due to the lack of initial assumptions needed to be made compared to classical optimization methods which require continuity and derivability of the objective function [2, 5, 9, 10]. To be able to optimize the airfoil a method of parameterization of the airfoil geometry is required. Well-behaved analytic functions are required due to the infinite slope at the leading edge of the airfoil. Several methods have been used to parametrize airfoils; these include Ferguson curves, Splines, Hicks-Henne bump functions, parametric Section (PARSEC) and Class/Shape function Transformation (CST). A comparison of these methods was done in [15].

In this article, the CST method is chosen due its intuitiveness and small number of variables required to describe the geometry and the PSO algorithm is used to design an airfoil. The optimized airfoil is then used for a preliminary design of a rotor; given some design, constraints on the tip chord the rotor radius and the blade root chord, with parameters that achieve the highest theoretical figure of merit. The rotor parameters are obtained using a combination of momentum theory and blade element theory. The figure of merit of an optimal propeller with the same geometric parameters is then compared using the optimized airfoil and the Clark Y airfoil.

2. Design Method

The airfoil geometry has a direct impact on its aerodynamic characteristics; hence, a reliable method of mathematically representing the airfoil geometry needs to be chosen. Kulfan developed a method of airfoil parameterization called Class function/Shape function Transformation (CST) [7], in which the airfoil is decomposed into two main functions: the class function (1) and the shape function (2). The shape function can be defined by using a series of Bernstein polynomials of any order (3).

$$C_{N2}^{N1} = (\psi)^{N1}(1-\psi)^{N2}, \tag{1}$$

$$S(\psi) = \sum_{i=0}^{N} A_i \psi^i, \tag{2}$$

$$S_i(\psi) = \frac{n!}{i!(n-i)!}\psi^i(1-\psi)^{n-i}, \tag{3}$$

where:
$\psi = x/c$,
C – airfoil chord,
n – Bernstein polynomial order,
A_i – coefficients that describe airfoil geometry,
$N1$, $N2$ – constants describing airfoil class.

The constants are chosen to be $N1 = 0.5$ and $N2 = 1.0$, which define a general class of airfoils. The overall geometry of the airfoil is then given by

$$(\xi)_{upper} = C_{N2}^{N1}(\psi)Su(\psi) + \psi\Delta\xi_u, \tag{4}$$

$$(\xi)_{lower} = C_{N2}^{N1}(\psi)Sl(\psi) + \psi\Delta\xi_l, \tag{5}$$

where:
ζ – thickness to chord ratio,
Su – upper surface shape function,
Sl – lower surface shape function.

The method of optimization plays an important role in the ability to find an optimum 2D airfoil within the search space. PSO was developed by Kennedy and Eberhart [6] to model the group dynamics of bird social behaviour. PSO is an evolutionary derivative-free optimization algorithm, which is preferred.

An amended form of the PSO algorithm uses a constriction factor χ to ensure convergence [4]. The amended system is described by

$$\boldsymbol{v}_i^{k+1} = \chi\left[\boldsymbol{v}_i^k + c_1 r_1\left(\boldsymbol{x}_{i,pb} - \boldsymbol{x}_i^k\right) + c_2 r_2\left(\boldsymbol{x}_{gb} - \boldsymbol{x}_i^k\right)\right], \tag{6a}$$

$$\boldsymbol{x}_i^{k+1} = \boldsymbol{x}_i^k + \boldsymbol{v}_i^{k+1}, \tag{6b}$$

$$\chi = \frac{2}{\left|\sqrt{2-\varphi-\sqrt{\varphi^2-4\varphi}}\right|}, \tag{6c}$$

where:
$\boldsymbol{v}_i^k$ – i-th particle velocity at the k-th iteration,
x_i^k – i-th particle position at the k-th iteration,
c_1 – social learning rate,
c_2 – cognitive learning rate,
r_1, r_2 – random numbers in the range [0,1],
$\boldsymbol{x}_{i,pb}$ – personal best position found by the i-th particle,
$\boldsymbol{x}_{gb}$ – global best position.

The conditions $\varphi = c_1 + c_2$, and $\varphi > 4$ should be met. The typical values used for the constants are obtained from [4, 14] with $c_1 = c_2 = 1.494$, $\varphi = 4.1$ and $\chi = 0.729$.

The particle positions and velocities are updated freely in the original PSO algorithm without any consideration for constraints. In airfoil optimization this can cause geometries that are unfeasible, to solve the problem the particles are confined within a “wall” within which a realizable geometry could be obtained. The constraint used is a semi-elastic wall in which the once the particle falls outside the constraint boundary the particle position and the velocity is updated using (7) [14].

$$\begin{aligned} &\text{if } x > x^{max}, \\ &\quad x = x^{max}, \\ &\quad v^{k+1} = -\frac{v^{k+1}}{\chi(c_1+c_2)}, \\ &\text{end} \\ &\text{if } x < x^{min}, \\ &\quad x = x^{min}, \\ &\quad v^{k+1} = -\frac{v^{k+1}}{\chi(c_1+c_2)}, \\ &\text{end.} \end{aligned} \tag{7}$$

In BEMT an annulus of the rotor disk is taken and the incremental thrust, dT, is calculated using momentum theory with the basic assumption that the individual annuli are independent on each other [8, 11, 16]. The assumption results in realistic results up until the blade tips due to various aerodynamic effects. To better approximate, the blade tips a Prandtl tip loss function is used to modify the inflow [8]. During hover the radial inflow equation is given by

$$\lambda(r) = \frac{\sigma(r)C_{l\alpha}}{16}\left(\sqrt{1 + \frac{32}{\sigma(r)C_{l\alpha}}\theta(r)r} - 1\right), \tag{8}$$

where:
$\lambda(r)$ – inflow at the radial station r,
$\sigma(r)$ – blade solidity at the radial station r,
$C_{l\alpha}$ – 2D lift slope curve of the airfoil,
$\theta(r)$ – blade twist at the radial station r.

The figure of merit, determines the efficiency of the rotor during hover, is given by the ratio of the ideal power required for hover and the actual power required for hover as given in

$$FoM = \frac{C_{P_{Ideal}}}{C_{P_i} + C_{P_0}}, \tag{9}$$

where:
$C_{P_{Ideal}}$ – ideal power coefficient,
C_{P_i} – induced power coefficient,
C_{P_0} – profile power coefficient.

To design the optimum hovering propeller, with the highest figure of merit, both the induced power and the profile power need to be minimized. To obtain a state that requires the minimum induced power the inflow needs to uniform over the disk, while for the minimum profile power each blade station on the rotor disk needs to operate at the airfoils maximum lift to drag ratio. To achieve this, the local solidity for the rotor is given by

$$\sigma(r) = \left(\frac{4C_T}{C_{l\alpha}\alpha_1}\right)\frac{1}{r}, \tag{10}$$

where:
C_T – thrust coefficient of the propeller,
α_1 – angle of attack at which the airfoil operates at the desired lift to drag ratio.
The optimum blade twist is then given by

$$\theta(r) = \alpha_1 + \frac{\lambda}{r}. \tag{11}$$

The total thrust coefficient C_T is found by numerically integrating the incremental thrust over the span of the propeller using the rectangle rule. As stated earlier there is a change in the inflow at the blade tips, the Prandtl tip loss function adds a correction factor F, which is used to find the new inflow and is described in

$$F = \left(\frac{2}{\pi}\right)\cos^{-1}(\exp(-f)), \tag{12a}$$

$$f = \frac{N_b}{2}\left(\frac{1-r}{r\phi}\right), \tag{12b}$$

where:
N_b – number of blades,
$\phi = \lambda/r$.
The modified inflow is then given by

$$\lambda(r) = \frac{\sigma(r)C_{l\alpha}}{16F}\left(\sqrt{1 + \frac{32F}{\sigma(r)C_{l\alpha}}\theta(r)r} - 1\right). \tag{13}$$

The correction factor, F, is a function of the inflow and thus cannot be computed immediately. An iterative procedure must be used by first calculating the inflow for in infinite number of blades $(F = 1)$ [8]. The incremental thrust at each blade station, ΔC_T, can then be obtained from

$$\Delta C_T = \frac{\sigma C_{l\alpha}}{2}(\theta(r)r^2 - \lambda(r)r)\Delta r. \tag{14}$$

Equation (14) can then be numerically integrated over the whole span of the propeller blade to obtain the propeller thrust coefficient C_T.

3. Experiments and results

As stated earlier, one of the ways to increase the figure of merit is by reducing the profile power of the rotor. Since the profile power is dependent on the airfoil lift to drag ratio, the PSO algorithm tries to minimize the negative lift to drag ratio with an angle of attack ranging from 0 to 6 degrees with increments of 1 degree. The cost function is given as follows

$$\min_{\alpha \in \mathbb{Z}|0 \le \alpha \le 6}\left(-\frac{C_l(\alpha)}{C_d(\alpha)}\right), \tag{15}$$

where:
α – airfoil angle of attack,

$C_l(\alpha)$ – airfoil lift coefficient,
$C_d(\alpha)$ – airfoil drag coefficient.

As stated earlier, one of the ways to increase the figure of merit is by reducing the profile power of the rotor. Since the profile power is dependent on the airfoil lift to drag ratio, the PSO algorithm tries to minimize the average negative lift to drag ratio with an angle of attack ranging from 0 to 6 degrees with increments of 1 degree.

Unlike the geometric constraints, which can be added to the PSO algorithm directly, the aerodynamic constraints need to be added by using a pseudo-cost function. The pseudo cost function consists of a penalty function, which is added to the original cost function. The penalty threshold and the penalties added to the cost function are given in Tab. 1.

To obtain the aerodynamic coefficients of the geometry, created using the CST method using parameters from the PSO algorithm, is loaded into XFOIL [3]. The output of XFOIL is a polar file containing the lift, drag and pitching moment coefficients at each angle of attack of the given geometry. The simulation is run with an angle of attack ranging from 0º to 6º with increments of 1°. The polar file is then read into MATLAB and together with calculations of the airfoil camber and thickness; the pseudo cost function is calculated.

The PSO algorithm initializes a random population of 30 airfoils with the minimum and maximum values for the coefficients given in Tab. 2. The trailing edge thickness for both the upper surface and lower surface were kept constant at 0.0025. The best airfoils cost function at each iteration and the lift to drag ratio of the optimized airfoil are shown in Fig. 1. Fig. 2 shows the lift and drag coefficients of the optimized airfoils with respect to the angle of attack. Fig. 3 presents the optimized airfoil shape and camber. The parameters of the optimized airfoil are presented in Tab. 3. The lift curve is assumed to be linear and is approximated by:

$$C_l = 6.53\alpha + 0.284. \tag{16}$$

The plot of the drag coefficient with respect to the angle of attack is shown in Fig. 6. The drag curve is assumed to be quadratic and is approximated by

$$C_d = 1.81\alpha^2 - 0.267\alpha + 0.0292. \tag{17}$$

Tab. 1. Cost function penalties for constraints

	Parameters			
	Drag Coefficient	*Pitching Moment Coefficient*	*Camber*	*Max Thickness*
Limits	< 0.15	$-0.1 < C_m < 0.1$	< 0.08	> 0.08
Penalty Value	10^5	10^2	10^4	10^4

Tab. 2. Airfoil shape function parameter limits

Limits	Parameters							
	Au_1	Au_2	Au_3	Au_4	Al_1	Al_2	Al_3	Al_4
min	0.1	–0.1	–0.1	–0.1	–0.2	–0.3	–0.3	–0.3
max	0.2	0.3	0.3	0.3	–0.1	0.1	0.1	0.1

Tab. 3. Optimized airfoil parameters

Parameters							
Au_1	Au_2	Au_3	Au_4	Al_1	Al_2	Al_3	Al_4
0.1713	0.2106	0.2304	0.2878	–0.1555	0.1388	–0.0436	–0.0313

The optimal hovering propeller is one at which the induced inflow is uniform over the span of the blade and that at each blade station the airfoil operates at the maximum lift to drag ratio [8].

The optimal propeller is designed using two different airfoils: the optimized airfoil and the Clark Y. Parameters of the Clark Y airfoil were obtained from [18].

The thrust coefficient for the optimized airfoil propeller is $C_T = 0.0061$ while the thrust coefficient for the Clark Y based propeller is $C_T = 0.0053$. The figure of merit for the optimized airfoil has a value $FoM = 0.6923$ while that of the Clark Y airfoil has a value of $FoM = 0.6683$.

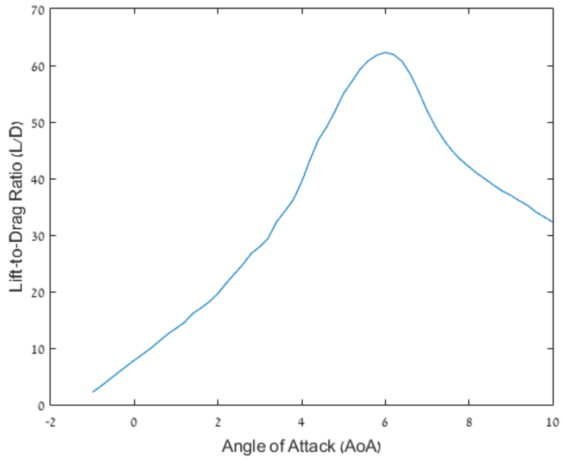

Fig. 1. Cost function vs iteration (left) and Lift to drag ratio vs angle of attack (right)

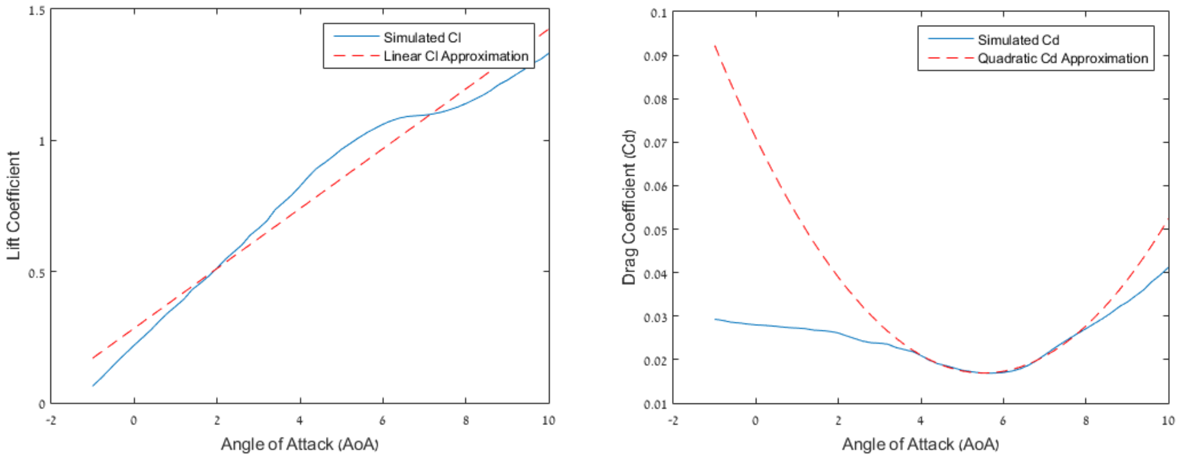

Fig. 2. Lift vs. angle of attack of optimized airfoil with linear approximation (left) and Drag vs. angle of attack with quadratic approximation (right)

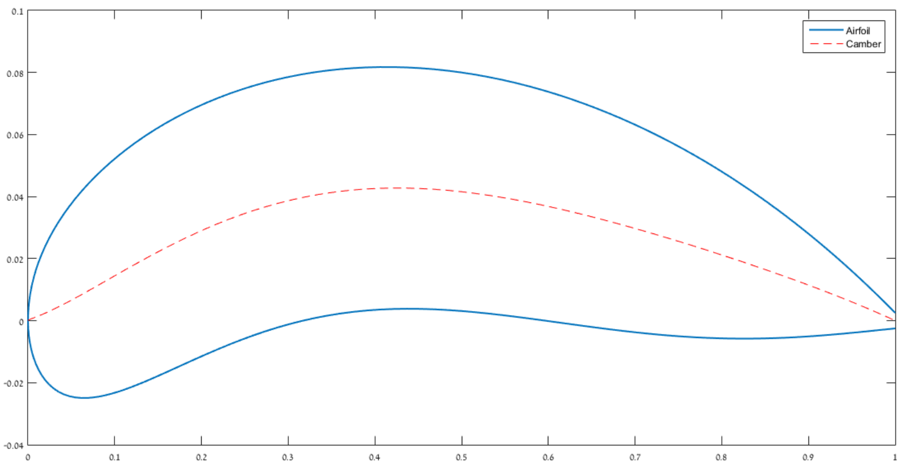

Fig. 3. Optimized airfoil

4. Conclusions

From the simulation results, it is evident that the PSO algorithm was able to find an airfoil that met all the design requirements. The lift-to-drag ratio was maximized and attained a value of 62.28, at an angle of attack of 6º. The Clark Y airfoil has a maximum lift-to-drag ratio of 53 at an angle of 6.75º. When used in the optimum hovering propeller the optimized airfoil attained a thrust coefficient of 0.0061 while the Clark Y attained 0.0053. The figure of merit of the optimized airfoil was 0.6923 while that of the Clark Y has a value of 0.6683. This results in only a slight increase of about 3% efficiency in hover. It should be noted that the linearized lift curve for the optimized airfoil was underestimated at its optimal angle of attack resulting in a lower value of than the true theoretical maximum figure of merit. Further research should be done using a higher order approximation of the optimized airfoil. The results should then be validated using a full CFD environment and finally a physical experiment should be realized to test the efficiency of the propeller with the optimized airfoil.

Acknowledgements

The work has been financially supported by the Polish Ministry of Science and Higher Education.

References

[1] Ambroziak, L., Gosiewski, Z., Kondratiuk, M., *Aerodynamics characteristics identification of micro air vehicle*, Transactions of the Institute of Aviation, No. 216, pp. 17-29, 2011.
[2] Carrese, R., Winatro, H., Watmuff, J., *User-preference particle swarm algorithm for airfoil design architecture*, in 27th Congress of the International Council of the Aeronautical Sciences, Nice 2010.
[3] Drela, M., *XFOIL: an analysis and design system for low Reynolds number airfoils*, Lecture Notes in Engineering, Vol. 54, pp. 1-12, 1989.
[4] Eberhart, R. C., Shi, Y., *Comparing inertia weights and constriction factors in particle swarm optimization*, Congress on Evolutionary Computation, San Diego, CA, Vol. 1, pp. 84-88, 2000.
[5] Helwig, S., Branke, J., Mostaghim, S., *Experimental analysis of bound handling techniques in particle swarm optimization*, IEEE Transactions on Evolutionary Computation, Vol. 17, No. 2, pp. 259-271, 2013.
[6] Kennedy, J., Eberhart, R. C., *Particle swarm optimization*, in IEEE International Conference on Neural Networks, Vol. 4, pp. 1942-1948, Perth, WA 1995.
[7] Kulfan, B., *Universal parametric geometry representation method*, Journal of Aircraft, Vol. 45, No. 1, pp. 142-158, 2008.
[8] Leishman, J., *Principles of helicopter aerodynamics*, 2nd ed., Cambridge Univ. Press, New York 2008.
[9] Ma, R., Zhong, B., Liu, P., Wang, W., *Multi-objective optimization design of low-Reynolds-number airfoil in Near Space*, 3rd International Symposium on Systems and Control in Aeronautics and Astronautics, 2010.
[10] Nemec, M., Zingg, D., Pulliam, T., *Multipoint and multi-objective aerodynamic shape optimization*, AIAA Journal, Vol. 42, Vo. 6, pp. 1057-1065, 2004.
[11] Prouty, R., *Helicopter performance, stability, and control*, 5th ed. Malabar: Krieger Pub., 2005.
[12] Ram, K., Lal, S., Ahmed M. R., *Low Reynolds number airfoil optimization for wind turbine applications using genetic algorithm*, Journal of Renewable and Sustainable Energy, Vol. 5, pp. 1-15, 2013.

[13] Ribeiro, A., Awruch, A., Gomes, H., *An airfoil optimization technique for wind turbines*, Applied Mathematical Modelling, Vol. 36, No. 10, pp. 4898-4907, 2012.
[14] Serani, A., Diez, M., Leotardi, C., Campana, E., *On the use of synchronous and asynchronous single-objective deterministic particle swarm optimization in ship design problems*, in 1st International Conference on Engineering and Applied Sciences Optimization, Kos 2014.
[15] Sripawadkul, V., Padulo, M., Guenov, M., *A comparison of airfoil shape parameterization techniques for early design optimization*, 13th AIAA/ISSMO Multidisciplinary Analysis Optimization Conference, 2010.
[16] Stepniewski, W., Keys, C., *Rotary-wing aerodynamics*, 1st ed., Dover Publ., New York 1984.
[17] Zyluk, A., Sibilski, K., Kowalski, M., Wisniowski, W., *Aerodynamic measurements micro air vehicle*, Journal of KONES Powertrain and Transport, Vol. 22, No. 4, pp. 343-353, 2015.
[18] M-selig.ae.illinois.edu. [online]. available: http://m-selig.ae.illinois.edu/ads/coord/clarky.dat.